SIAM J. NUMER. ANAL.
Vol. 39, No. 1, pp. 264–285


# SUPERCONVERGENCE OF THE LOCAL DISCONTINUOUS GALERKIN METHOD FOR ELLIPTIC PROBLEMS ON CARTESIAN GRIDS*

BERNARDO COCKBURN†, GUIDO KANSCHAT‡, ILARIA PERUGIA§, AND DOMINIK SCHÖTZAU†

**Abstract.** In this paper, we present a superconvergence result for the local discontinuous Galerkin (LDG) method for a model elliptic problem on Cartesian grids. We identify a *special* numerical flux for which the $L^2$-norm of the gradient and the $L^2$-norm of the potential are of orders $k + 1/2$ and $k + 1$, respectively, when tensor product polynomials of degree at most $k$ are used; for arbitrary meshes, this special LDG method gives only the orders of convergence of $k$ and $k + 1/2$, respectively. We present a series of numerical examples which establish the sharpness of our theoretical results.

**Key words.** finite elements, discontinuous Galerkin methods, superconvergence, elliptic problems, Cartesian grids

**AMS subject classification.** 65N30

**PII.** S0036142900371544

## 1. Introduction.

In this paper, we derive a priori error estimates of the local discontinuous Galerkin (LDG) method on Cartesian grids for the following classical model elliptic problem:

$$\begin{aligned} -\Delta u &= f && \text{in } \Omega, \\ u &= g_{\mathcal{D}} && \text{on } \Gamma_{\mathcal{D}}, \\ \nabla u \cdot \boldsymbol{n} &= \boldsymbol{g}_{\mathcal{N}} \cdot \boldsymbol{n} && \text{on } \Gamma_{\mathcal{N}}, \end{aligned} \tag{1.1}$$

where $\Omega$ is a bounded domain of $\mathbb{R}^d$, $d = 2, 3$, and $\boldsymbol{n}$ is the outward unit normal to its boundary $\Gamma = \overline{\Gamma}_{\mathcal{D}} \cup \overline{\Gamma}_{\mathcal{N}}$; we assume that the $(d-1)$-measure of $\Gamma_{\mathcal{D}}$ is nonzero.

This paper is a natural continuation of the work done in [3] by Castillo, Cockburn, Perugia, and Schötzau where the first a priori error analysis of the LDG method for purely elliptic problems was carried out. Meshes consisting of elements of various shapes and with hanging nodes were considered and general numerical fluxes were studied. It was shown that, for smooth solutions, the orders of convergence of the $L^2$-norms of the errors in $\nabla u$ and in $u$ are $k$ and $k + 1/2$, respectively, when polynomials

*Received by the editors April 27, 2000; accepted for publication (in revised form) September 26, 2000; published electronically March 7, 2001.
http://www.siam.org/journals/sinum/39-1/37154.html

†School of Mathematics, University of Minnesota, Vincent Hall, Minneapolis, MN 55455 (cockburn@math.umn.edu, schoetza@math.umn.edu). The first author was supported in part by the National Science Foundation (grant DMS-9807491) and by the University of Minnesota Supercomputing Institute. The fourth author was supported by the Swiss National Science Foundation (Schweizerischer Nationalfonds).

‡Institut für Angewandte Mathematik, Universität Heidelberg, INF 293/294, 69120 Heidelberg, Germany (guido.kanschat@na-net.ornl.gov). This author was supported in part by the ARO DAAG55-98-1-0335 and by the University of Minnesota Supercomputing Institute. This work was carried out when the author was a visiting professor at the School of Mathematics, University of Minnesota.

§Dipartimento di Matematica, Università di Pavia, Via Ferrata 1, 27100 Pavia, Italy (perugia@dimat.unipv.it). This author was supported in part by the Consiglio Nazionale delle Ricerche. This work was carried out when the author was a visiting professor at the School of Mathematics, University of Minnesota.

of degree at most $k$ are used. On the other hand, Castillo [2] and then Castillo, Cockburn, Schötzau, and Schwab [4] proved a superconvergence result for one-space dimension transient convection-diffusion problems, namely, that the optimal order of convergence of the error in the energy norm, $k+1$, can actually be obtained *provided* that the so-called numerical fluxes are suitably chosen. In this paper, we *extend* these results to the LDG method on Cartesian grids for the multidimensional elliptic model problem (1.1). We show that the orders of convergence in the $L^2$-norm of the error in $\nabla u$ and $u$ are $k+1/2$ and $k+1$, respectively, when tensor product polynomials of degree at most $k$ are used. Our proof of this superconvergence result is a modification of the analysis carried out in [3]; it takes advantage of the Cartesian structure of the grid and makes use of a key idea introduced by LeSaint and Raviart [8] in their study of the original DG method for steady-state linear transport.

Since our analysis is a special modification of that of [3], in order to avoid unnecessary repetitions, we refer the reader to [3] for a more detailed description of the framework of our error analysis. The organization of this paper is as follows. In section 2, we briefly display the LDG method in compact form, introduce the special numerical flux on Cartesian grids, and present and discuss our main results. In section 3, the detailed proofs are given, and in section 4 we present several numerical experiments showing the optimality of our theoretical results. We end in section 5 with some concluding remarks.

**2. The main results.** In this section we recall the formulation of the LDG method and identify the special numerical flux we are going to investigate on Cartesian grids. Then we state and discuss our main results. As pointed out in the introduction, we refer to [3] for more details concerning the formulation of the LDG method.

**2.1. The LDG method.** To introduce the LDG method, we rewrite our elliptic model problem (1.1) as the following system of first-order equations:

$$\boldsymbol{q} = \nabla u \qquad \text{in } \Omega, \tag{2.1}$$

$$-\nabla \cdot \boldsymbol{q} = f \qquad \text{in } \Omega, \tag{2.2}$$

$$u = g_{\mathcal{D}} \qquad \text{on } \Gamma_{\mathcal{D}}, \tag{2.3}$$

$$\boldsymbol{q} \cdot \boldsymbol{n} = \boldsymbol{g}_{\mathcal{N}} \cdot \boldsymbol{n} \qquad \text{on } \Gamma_{\mathcal{N}}. \tag{2.4}$$

To obtain the weak formulation with which the LDG method is defined, we multiply (2.1) and (2.2) by arbitrary, smooth test functions $\boldsymbol{r}$ and $v$, respectively, and integrate by parts over the $d$-dimensional rectangle $K$ of the Cartesian grid $\mathcal{T}$ with which we triangulate the domain $\Omega$. Then we replace the exact solution $(\boldsymbol{q}, u)$ by its approximation $(\boldsymbol{q}_N, u_N)$ in the finite element space $\boldsymbol{M}_N \times V_N$, where

$$\boldsymbol{M}_N := \{\boldsymbol{q} \in (L^2(\Omega))^d \ : \ \boldsymbol{q}\big|_K \in \mathcal{S}(K)^d, \ \forall K \in \mathcal{T}\}, \tag{2.5}$$

$$V_N \ := \{u \in L^2(\Omega) \ : \ u\big|_K \in \mathcal{S}(K), \ \forall K \in \mathcal{T}\}, \tag{2.6}$$

and

$$\mathcal{S}(K) := \mathcal{Q}^k(K) = \{\text{polynomials of degree at most } k \text{ in each variable on } K\}.$$

The method consists in finding $(\boldsymbol{q}_N, u_N) \in \boldsymbol{M}_N \times V_N$ such that

$$\int_K \boldsymbol{q}_N \cdot \boldsymbol{r} \, d\boldsymbol{x} = -\int_K u_N \, \nabla \cdot \boldsymbol{r} \, d\boldsymbol{x} + \int_{\partial K} \widehat{u}_N \, \boldsymbol{r} \cdot \boldsymbol{n}_{\boldsymbol{K}} \, ds, \tag{2.7}$$

$$\int_K \boldsymbol{q}_N \cdot \nabla v \, d\boldsymbol{x} = \int_K f v \, d\boldsymbol{x} + \int_{\partial K} v \, \widehat{\boldsymbol{q}}_N \cdot \boldsymbol{n}_{\boldsymbol{K}} \, ds, \tag{2.8}$$

for all test functions $(\boldsymbol{r}, v) \in S(K)^d \times S(K)$, for all elements $K \in \mathcal{T}$; here, $\boldsymbol{n}_K$ denotes the unit outward normal to $\partial K$. The functions $\widehat{u}_N$ and $\widehat{\boldsymbol{q}}_N$ in (2.7) and (2.8) are the so-called *numerical fluxes*. These are nothing but discrete approximations to the traces of $u$ and $\boldsymbol{q}$ on the boundary of the elements. To define these numerical fluxes, we need to introduce some notation. Let $K^+$ and $K^-$ be two adjacent elements of $\mathcal{T}$; let $\boldsymbol{x}$ be an arbitrary point of the $(d-1)$-dimensional face $e = \partial K^+ \cap \partial K^-$, and let $\boldsymbol{n}^+$ and $\boldsymbol{n}^-$ be the corresponding outward unit normals at that point. Let $(\boldsymbol{q}, u)$ be a function smooth inside each element $K^\pm$, and let us denote by $(\boldsymbol{q}^\pm, u^\pm)$ the traces of $(\boldsymbol{q}, u)$ on $e$ from the interior of $K^\pm$. Then, we define the mean values $\{\!\{\cdot\}\!\}$ and jumps $[\![\cdot]\!]$ at $\boldsymbol{x} \in e$ as follows:

$$\{\!\{u\}\!\} := (u^+ + u^-)/2, \qquad \{\!\{\boldsymbol{q}\}\!\} := (\boldsymbol{q}^+ + \boldsymbol{q}^-)/2,$$
$$[\![u]\!] := u^+\boldsymbol{n}^+ + u^-\boldsymbol{n}^-, \qquad [\![\boldsymbol{q}]\!] := \boldsymbol{q}^+ \cdot \boldsymbol{n}^+ + \boldsymbol{q}^- \cdot \boldsymbol{n}^-.$$

We are now ready to introduce the expressions that define the numerical fluxes in (2.7) and (2.8). If $e$ is inside the domain $\Omega$, we take

$$\begin{aligned} \widehat{\boldsymbol{q}} &:= \{\!\{\boldsymbol{q}\}\!\} - C_{11}[\![u]\!] - \boldsymbol{C}_{12}[\![\boldsymbol{q}]\!], \\ \widehat{u} &:= \{\!\{u\}\!\} + \boldsymbol{C}_{12} \cdot [\![u]\!], \end{aligned} \tag{2.9}$$

and, if $e$ lies on the boundary of $\Omega$,

$$\widehat{\boldsymbol{q}} := \begin{cases} \boldsymbol{q}^+ - C_{11}(u^+ - g_{\mathcal{D}})\boldsymbol{n} & \text{on } \Gamma_{\mathcal{D}}, \\ \boldsymbol{g}_{\mathcal{N}} & \text{on } \Gamma_{\mathcal{N}} \end{cases} \qquad \text{and} \qquad \widehat{u} := \begin{cases} g_{\mathcal{D}} & \text{on } \Gamma_{\mathcal{D}}, \\ u^+ & \text{on } \Gamma_{\mathcal{N}}. \end{cases} \tag{2.10}$$

Moreover, the stabilization parameter $C_{11}$ and the auxiliary parameter $\boldsymbol{C}_{12}$ are defined on each face $e$ as follows:

$$C_{11}(e) = \zeta, \qquad \boldsymbol{C}_{12}(e) \cdot \boldsymbol{n} = \operatorname{sign}(\boldsymbol{v} \cdot \boldsymbol{n})/2, \tag{2.11}$$

where $\zeta$ is a positive real number independent of the mesh size (and chosen as $\zeta = 1.0$ in all our numerical experiments), and $\boldsymbol{v}$ is an arbitrary but fixed vector $\boldsymbol{v}$ with nonzero components. Note that with this choice of the parameter $\boldsymbol{C}_{12}(e)$, we have that

$$\widehat{u} = \frac{1}{2}(1 + \operatorname{sign}(\boldsymbol{v} \cdot \boldsymbol{n}))\, u^+ + \frac{1}{2}(1 - \operatorname{sign}(\boldsymbol{v} \cdot \boldsymbol{n}))\, u^-,$$

that is, if $\boldsymbol{v}$ is the vector displayed in Figure 3.1, we have that on the vertical edges, $\widehat{u}$ is *always* equal to the left trace of $u$, and on the horizontal edges, $\widehat{u}$ is *always* equal to the trace of $u$ from below. Similarly, $\{\!\{\boldsymbol{q}\}\!\} - \boldsymbol{C}_{12}[\![\boldsymbol{q}]\!]$ is equal to the right trace of $\boldsymbol{q}$ on the vertical edges and the trace of $\boldsymbol{q}$ from above on the horizontal edges. In other words, the role of the vector $\boldsymbol{v}$ is to give a single rule to pick the numerical fluxes $\widehat{u}$ and $\boldsymbol{q}$ for all the elements; this is the only relevant property of the choice of the auxiliary vector $\boldsymbol{v}$.

**2.2. Error analysis on Cartesian grids.** To state our main result, we need to recall some notation and to introduce additional hypotheses. We restrict our analysis to domains $\Omega$ such that, when $f$ is in $\mathrm{L}^2(\Omega)$ and the boundary data are zero, we have $u \in H^2(\Omega)$ and the elliptic regularity result $\| u \|_2 \le C \| f \|_0$.

We denote by $h_K$ the diameter of an element $K$ and set, as usual, $h := \max_{K \in \mathcal{T}} h_K$. We denote by $\mathcal{E}_{\mathcal{I}}$ the set of all interior faces of the triangulation $\mathcal{T}$, by $\mathcal{E}_{\mathcal{D}}$ the set

of faces on $\Gamma_{\mathcal{D}}$, and by $\mathcal{E}_{\mathcal{N}}$ the set of faces on $\Gamma_{\mathcal{N}}$; we assume that $\overline{\Gamma}_{\mathcal{D}} = \cup_{e\in\mathcal{E}_{\mathcal{D}}}\overline{e}$ and $\overline{\Gamma}_{\mathcal{N}} = \cup_{e\in\mathcal{E}_{\mathcal{N}}}\overline{e}$. The Cartesian triangulations we consider do not contain hanging nodes and are shape-regular, that is, if $\rho_K$ denotes the radius of the biggest ball included in $K$, we have

$$\frac{h_K}{\rho_K} \leq \sigma \qquad \forall K \in \mathcal{T} \tag{2.12}$$

with a positive constant $\sigma$. Moreover, we denote by $E_{\mathcal{N}} \subset \overline{\Omega}$ a closed set containing the intersection between the Neumann boundary $\Gamma_{\mathcal{N}}$ and the set $\Gamma^- := \{\boldsymbol{x} \in \Gamma : \boldsymbol{v}\cdot\boldsymbol{n}(\boldsymbol{x}) < 0\}$. We assume that the triangulation $\mathcal{T}$ is such that

$$\bigcup_{e\subset\Gamma_{\mathcal{N}}\cap\Gamma^-} K_e \subset E_{\mathcal{N}}, \tag{2.13}$$

where $K_e$ denotes, from now on, an element containing the face $e$. Finally, we introduce the seminorm $|\,(\boldsymbol{q},u)\,|_{\mathcal{A}}^2$ that appears in a natural way in the analysis of the LDG method and is defined as

$$|\,(\boldsymbol{q},u)\,|_{\mathcal{A}}^2 := \|\,\boldsymbol{q}\,\|_0^2 + \sum_{e\in\mathcal{E}_{\mathcal{I}}}\int_e C_{11}\,[\![u]\!]^2\,ds + \sum_{e\in\mathcal{E}_{\mathcal{D}}}\int_e C_{11}\,u^2\,ds. \tag{2.14}$$

We are now ready to state our main result.

THEOREM 2.1. *Assume that the solution* $(\boldsymbol{q},u)$ *of* (2.1)–(2.4) *belongs to* $H^{k+1}(\Omega)^d \times H^{k+2}(\Omega)$ *for* $k \geq 0$. *If the intersection between* $\Gamma_{\mathcal{N}}$ *and* $\Gamma^-$ *is nonempty, we assume, furthermore, that* $u$ *belongs to* $W^{k+1,\infty}(E_{\mathcal{N}})$. *Assume that the Cartesian grid* $\mathcal{T}$ *is shape-regular,* (2.12), *and that it satisfies the condition* (2.13) *if* $\Gamma_{\mathcal{N}}\cap\Gamma^- \neq \emptyset$. *Let* $(\boldsymbol{q}_N,u_N) \in \boldsymbol{M}_N \times V_N$ *be the approximation of* $(\boldsymbol{q},u)$ *given by the* LDG *method with* $k \geq 0$ *and numerical fluxes defined by* (2.9), (2.10), *and* (2.11).

*Then we have*

$$\|u-u_N\|_0 \leq Ch^{k+1}$$

*and*

$$|\,(\boldsymbol{q}-\boldsymbol{q}_N, u-u_N)\,|_{\mathcal{A}} \leq Ch^{k+\frac{1}{2}},$$

*where the constant* $C$ *depends solely on* $\Omega$, $\zeta$, $k$, $d$, $\sigma$, $\|\,u\,\|_{k+2}$ *and on* $\|\,u\,\|_{W^{k+1,\infty}(E_{\mathcal{N}})}$ *if* $\Gamma_{\mathcal{N}}\cap\Gamma^- \neq \emptyset$.

Several important remarks are in order before we prove this result in the next section.

*Remark* 2.2. The error bounds in Theorem 2.1 improve the results in [3] by a factor $\sqrt{h}$. However, they just hold on Cartesian grids and for the particular choice of $\boldsymbol{C}_{12}$ in (2.11). Moreover, their proof requires stronger smoothness assumptions on the exact solution than the ones considered in [3]. In this sense, Theorem 2.1 is a superconvergence result. It can be considered as an extension to the bounded domain case of the corresponding result by Cockburn and Shu [7] for the LDG method for transient convection-diffusion problems. It is also an extension to the multidimensional case of the results obtained by Castillo, Cockburn, Schötzau, and Schwab [4] in the one-space dimension case. The key ingredient of its proof is a superconvergence result similar to the one LeSaint and Raviart used in their study of the original DG method for steady-state linear transport in Cartesian grids [8].

*Remark* 2.3. Note that Theorem 2.1 holds true in the case $k = 0$, that is, when the approximate solution is piecewise constant. In [3], all the error estimates obtained for the corresponding LDG method on general grids are valid only for $k \geq 1$; moreover, no order of convergence is numerically observed for $k = 0$.

*Remark* 2.4. From an approximation point of view, the order of convergence in $\boldsymbol{q}$, namely, $k+1/2$, is suboptimal by one-half; however, it is confirmed to be sharp by our numerical experiments in section 4. For general numerical fluxes and unstructured grids, an order of convergence in $\boldsymbol{q}$ of only $k$ is obtained; see [3].

*Remark* 2.5. If we consider the more general case where the coefficients $C_{11}$ are chosen mesh-dependent and given in the form

$$C_{11}(e) = \zeta \begin{cases} \min\{h_{K_e^+}^{\alpha}, h_{K_e^-}^{\alpha}\} & \text{if } K_e^+ \cap K_e^- = e, \\ h_{K_e}^{\alpha} & \text{if } e \subset \Gamma \end{cases} \tag{2.15}$$

with constants $\zeta > 0$ and $\alpha \in [-1, 1]$ independent of the mesh size, we might conceive the possibility that a suitable tuning of the value of $\alpha$ could improve the order of convergence in $\boldsymbol{q}$. However, this is not true, as will be made clear in the proof of Theorem 2.1 displayed in the next section, and in the numerical results of subsection 4.2. See also [3] for other results about the influence of the value of $\alpha$ on the orders of convergence of the general LDG method.

*Remark* 2.6. In Theorem 2.1, an extra regularity condition on the exact solution $u$ on the closed set $E_{\mathcal{N}}$ containing part of the Neumann boundary is required. If this condition is dropped, and if $\Gamma_{\mathcal{N}} \cap \Gamma^-$ is not empty, only an order of convergence of $k$ in the error in $\boldsymbol{q}$ can be proved by using our technique, which represents a loss of one-half. Note that whenever it is possible to choose $\boldsymbol{v}$ in such a way that $\Gamma_{\mathcal{N}} \cap \Gamma^- = \emptyset$, no extra regularity assumption on the exact solution is required.

*Remark* 2.7. The set $\Gamma^-$ depends on the choice of the vector $\boldsymbol{v}$. As it will become clear in the proof, the only way the constant $C$ in Theorem 2.1 depends on $\boldsymbol{v}$ is through $\| u \|_{W^{k+1,\infty}(E_{\mathcal{N}})}$ if $\Gamma_{\mathcal{N}} \cap \Gamma^- \neq \emptyset$. Hence, whenever $\boldsymbol{v}$ can be chosen in such a way that $\Gamma_{\mathcal{N}} \cap \Gamma^- = \emptyset$, $C$ is independent of $\boldsymbol{v}$; in particular, the estimates are totally independent of the auxiliary vector $\boldsymbol{v}$ when the boundary conditions are Dirichlet since then $\Gamma_{\mathcal{N}} = \emptyset$.

**3. Proofs.** This section is devoted to the proof of Theorem 2.1. For simplicity, we consider only the case $d = 2$, $\Omega$ rectangle, and the choice of $\boldsymbol{v}$ as in Figure 3.1. All the arguments we present in our analysis rely on tensor product structures and can be easily extended to the case $d = 3$. We must point out, however, that a subtle smoothness requirement for the definition of the auxiliary projections we use prevents a straightforward extension of the analysis to the case $d > 3$; see subsection 3.2 for details.

To prove Theorem 2.1, we follow the approach used by [3]. Thus, we start, in subsection 3.1, by briefly reviewing the setting of our error analysis. We proceed in subsection 3.2 by introducing the projections $\boldsymbol{\Pi}$ and $\Pi$ which generalize to several space dimensions the projections used by Castillo, Cockburn, Schötzau, and Schwab [4] in their study of the LDG method for transient convection-diffusion problems in one-space dimension. Then, in subsection 3.3, we derive the expressions of the functionals $K_{\mathcal{A}}$ and $K_{\mathcal{B}}$ needed in the setting of [3] to get error estimates. To do so, we make use of a superconvergence result essentially due to LeSaint and Raviart [8] whose proof is presented in subsection 3.4. The proof of Theorem 2.1 is completed in subsection 3.5.

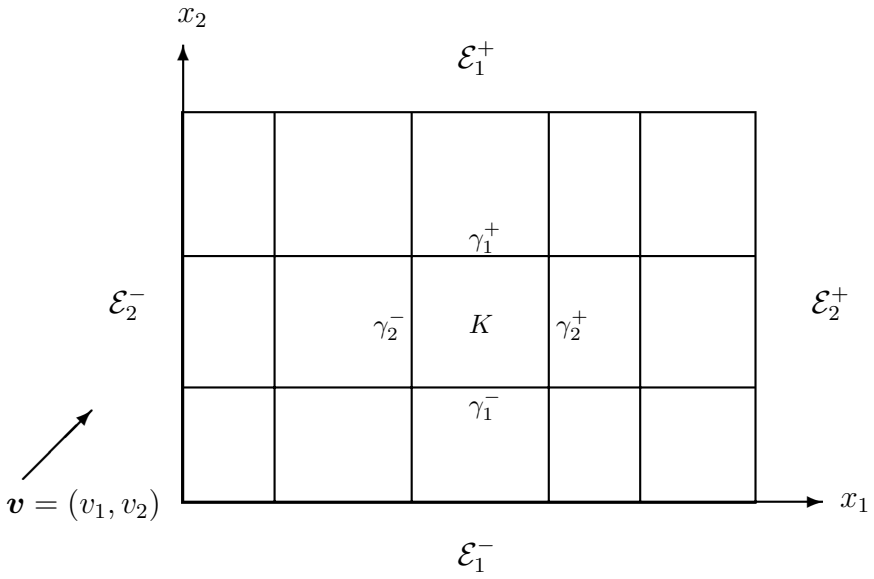


FIG. 3.1. *The Cartesian grid $\mathcal{T}$ and the auxiliary vector $\boldsymbol{v}$ used to define the numerical fluxes.*

**3.1. The framework of the error analysis.** All the following results are collected from [3]. First, we begin by reviewing that, by summation over all elements, the LDG method can be written in the following compact form. Find $(\boldsymbol{q}_N, u_N) \in \boldsymbol{M}_N \times V_N$ such that

$$\mathcal{A}(\boldsymbol{q}_N, u_N; \boldsymbol{r}, v) = \mathcal{F}(\boldsymbol{r}, v) \qquad \forall (\boldsymbol{r}, v) \in \boldsymbol{M}_N \times V_N,$$

by setting

$$\begin{aligned} \mathcal{A}(\boldsymbol{q}, u; \boldsymbol{r}, v) &:= a(\boldsymbol{q}, \boldsymbol{r}) + b(u, \boldsymbol{r}) - b(v, \boldsymbol{q}) + c(u, v), \\ \mathcal{F}(\boldsymbol{r}, v) &:= F(\boldsymbol{r}) + G(v) \end{aligned}$$

with

$$\begin{aligned} a(\boldsymbol{q}, \boldsymbol{r}) &:= \int_\Omega \boldsymbol{q} \cdot \boldsymbol{r}\, d\boldsymbol{x}, \\ b(u, \boldsymbol{r}) &:= \sum_{K \in \mathcal{T}} \int_K u \nabla \cdot \boldsymbol{r}\, d\boldsymbol{x} - \sum_{e \in \mathcal{E}_\mathcal{I}} \int_e (\{\!\{u\}\!\} + \boldsymbol{C}_{12} \cdot [\![u]\!])\, [\![\boldsymbol{r}]\!]\, ds - \sum_{e \in \mathcal{E}_\mathcal{N}} \int_e u\, \boldsymbol{r} \cdot \boldsymbol{n}\, ds, \\ c(u, v) &:= \sum_{e \in \mathcal{E}_\mathcal{I}} \int_e C_{11}\, [\![u]\!] \cdot [\![v]\!]\, ds + \sum_{e \in \mathcal{E}_\mathcal{D}} \int_e C_{11}\, uv\, ds. \end{aligned}$$

The linear forms $F$, $G$ are defined by

$$\begin{aligned} F(\boldsymbol{r}) &:= \sum_{e \in \mathcal{E}_\mathcal{D}} \int_e g_\mathcal{D}\, \boldsymbol{r} \cdot \boldsymbol{n}\, ds, \\ G(v) &:= \int_\Omega f v\, d\boldsymbol{x} + \sum_{e \in \mathcal{E}_\mathcal{D}} \int_e C_{11}\, g_\mathcal{D} v\, ds + \sum_{e \in \mathcal{E}_\mathcal{N}} \int_e v\, \boldsymbol{g}_\mathcal{N} \cdot \boldsymbol{n}\, ds. \end{aligned}$$

To prove error estimates for the LDG method, we follow [3]. We introduce two functionals, $K_{\mathcal{A}}$ and $K_{\mathcal{B}}$, which capture the approximation properties of the LDG method; the functionals are related to two suitably chosen projections $\mathbf{\Pi}$ and $\Pi$ onto the finite element (FE) spaces $\boldsymbol{M}_N$ and $V_N$, respectively. Namely, we require $K_{\mathcal{A}}$ and $K_{\mathcal{B}}$ to satisfy

$$|\,\mathcal{A}(\boldsymbol{q}-\mathbf{\Pi}\boldsymbol{q},u-\Pi u;\mathbf{\Phi}-\mathbf{\Pi}\mathbf{\Phi},\varphi-\Pi\varphi)\,|\le K_{\mathcal{A}}(\boldsymbol{q},u;\mathbf{\Phi},\varphi) \tag{3.1}$$

for any $(\boldsymbol{q},u)$, $(\mathbf{\Phi},\varphi)\in H^1(\Omega)^d\times H^2(\Omega)$ and

$$|\,\mathcal{A}(\boldsymbol{r},v;\boldsymbol{q}-\mathbf{\Pi}\boldsymbol{q},u-\Pi u)\,|\le|\,(\boldsymbol{r},v)\,|_{\mathcal{A}}\,K_{\mathcal{B}}(\boldsymbol{q},u) \tag{3.2}$$

for any $(\boldsymbol{r},v)\in\boldsymbol{M}_N\times V_N$ and $(\boldsymbol{q},u)\in H^1(\Omega)^d\times H^2(\Omega)$, where the $\mathcal{A}$-seminorm is defined in (2.14).

By Galerkin orthogonality, all the error estimates can then be expressed solely in terms of $K_{\mathcal{A}}$ and $K_{\mathcal{B}}$ as can be seen in the following result.

LEMMA 3.1 (cf. [3]). *We have*

$$|\,(\boldsymbol{q}-\boldsymbol{q}_N,u-u_N)\,|_{\mathcal{A}}\le K_{\mathcal{A}}^{1/2}(\boldsymbol{q},u;\boldsymbol{q},u)+K_{\mathcal{B}}(\boldsymbol{q},u).$$

*Furthermore,*

$$\|\,u-u_N\,\|_0\le\sup_{\lambda\in L^2(\Omega)}\frac{K_{\mathcal{A}}(\boldsymbol{q},u;\mathbf{\Phi},\varphi)}{\|\,\lambda\,\|_0}+K_{\mathcal{B}}(\boldsymbol{q},u)\sup_{\lambda\in L^2(\Omega)}\frac{K_{\mathcal{B}}(\mathbf{\Phi},\varphi)}{\|\,\lambda\,\|_0}$$

*with $\varphi$ denoting the solution of the adjoint problem*

$$\begin{aligned}-\Delta\varphi&=\lambda &&\text{in }\Omega,\\ \varphi&=0 &&\text{on }\Gamma_{\mathcal{D}},\\ \frac{\partial\varphi}{\partial n}&=0 &&\text{on }\Gamma_{\mathcal{N}},\end{aligned}$$

*and $\mathbf{\Phi}=-\nabla\varphi$.*

**3.2. Projections.** In this subsection, we define the projections $\mathbf{\Pi}$ and $\Pi$ we are going to use in the setting of subsection 3.1 to prove Theorem 2.1 and list their properties. We start by introducing the projections $\mathbf{\Pi}^{\pm}$ and $\Pi^{\pm}$ in terms of which the projections $\mathbf{\Pi}$ and $\Pi$ will then be defined according to the choice of the auxiliary vector $\boldsymbol{v}$ in (2.11).

In order to define $\Pi^{\pm}$, we have to introduce some one-dimensional projections. Let $I=(a^-,a^+)$ be an arbitrary interval, and let $\mathcal{P}^k(I)$ be the space of the polynomials of degree at most $k$ on $I$. We denote by $\pi$ the $\mathrm{L}^2(I)$-projection onto $\mathcal{P}^k(I)$, i.e., for a function $w\in\mathrm{L}^2(I)$ the projection $\pi w$ is the unique polynomial in $\mathcal{P}^k(I)$ satisfying

$$\int_I[w(x)-\pi w(x)]\,p(x)\,dx=0\qquad\forall p\in\mathcal{P}^k(I).$$

Furthermore, for $w\in H^{\frac12+\varepsilon}(I)$, we define the projections $\pi^{\pm}w\in\mathcal{P}^k(I)$ by the following $k+1$ conditions:

$$\int_I[w(x)-\pi^{\pm}w(x)]\,p(x)\,dx=0\qquad\forall p\in\mathcal{P}^{k-1}(I),\qquad\pi^{\pm}w(a^{\pm})=w(a^{\pm}).$$

On a rectangle $K = I_1 \times I_2$, for $v \in C^0(\overline{K})$, we define

$$\Pi^{\pm} v := \pi_1^{\pm} \otimes \pi_2^{\pm} v \tag{3.3}$$

with the subscripts indicating the application of the one-dimensional operators $\pi$ or $\pi^{\pm}$ with respect to the corresponding variable. Since $H^2(K)$ and $W^{1,\infty}(K)$ are embedded in $C^0(\overline{K})$, for $d = 2$ and $d = 3$ (see, e.g., [5, p. 114]), $\Pi^{\pm} v$ in (3.3) is well defined for $v \in H^2(K)$ and $v \in W^{1,\infty}(K)$. However, for $d > 3$, the first embedding is not true and the projections $\Pi^{\pm}$ are not well defined anymore for $v \in H^2(K)$; this is the technical detail that prevents a straightforward extension of our analysis to the case $d > 3$.

With the notation indicated in Figure 3.1, for $\boldsymbol{r} \in H^1(K)^2$, we define $\boldsymbol{\Pi}^{\pm} \boldsymbol{r} \in \mathcal{Q}^k(K)^2$ by

$$\int_K [\boldsymbol{r} - \boldsymbol{\Pi}^{\pm} \boldsymbol{r}] \cdot \nabla p \, d\boldsymbol{x} = 0 \qquad \forall p \in \mathcal{Q}^k(K), \tag{3.4}$$

$$\int_{\gamma_i^{\pm}} [\boldsymbol{r} - \boldsymbol{\Pi}^{\pm} \boldsymbol{r}] \cdot \boldsymbol{n} \, p \, ds = 0 \qquad \forall p \in \mathcal{Q}^k(\gamma_i^{\pm}), \quad i = 1, 2. \tag{3.5}$$

It can be easily seen that the conditions in (3.4) and (3.5) actually define $\boldsymbol{\Pi}^{\pm} \boldsymbol{r}$ in a unique way. Note that, whenever $\boldsymbol{r}$ is smoother than merely belonging to $H^1(K)^2$, $\boldsymbol{\Pi}^{\pm} \boldsymbol{r}$ defined by (3.4) and (3.5) can be represented as

$$\boldsymbol{\Pi}^{\pm} \boldsymbol{r} = (\pi_1^{\pm} \otimes \pi_2 r_1, \pi_1 \otimes \pi_2^{\pm} r_2). \tag{3.6}$$

Finally, we define the projections $\boldsymbol{\Pi}$ and $\Pi$. To do that, we must take into account the choice of the auxiliary vector $\boldsymbol{v}$ since the analysis shows that it is essential to have

$$\begin{aligned} &\widehat{u}_N = \Pi u_N\big|_K \text{ on } e \subset \partial K : \boldsymbol{v} \cdot \boldsymbol{n}_K|_e > 0, \\ &\{\!\{\boldsymbol{q}\}\!\} - \boldsymbol{C}_{12} [\![\boldsymbol{q}]\!] = \boldsymbol{\Pi} \boldsymbol{q}_N\big|_K \text{ on } e \subset \partial K : \boldsymbol{v} \cdot \boldsymbol{n}_K|_e < 0. \end{aligned}$$

For $\boldsymbol{v}$ as in Figure 3.1, we must take

$$\boldsymbol{\Pi} \boldsymbol{q}_{|K} := \boldsymbol{\Pi}^{-} \boldsymbol{q}_{|K}, \qquad \Pi u_{|K} := \Pi^{+} u_{|K}, \qquad \forall K \in \mathcal{T}. \tag{3.7}$$

This is the choice we shall use from now on.

In our analysis, we need several approximation results which we gather in the lemma below.

LEMMA 3.2. *Let $v \in H^{s+2}(K)$ and $\boldsymbol{r} \in H^{s+1}(K)^2$, $s \geq 0$. Then for $m = 0, 1$, we have*

$$|v - \Pi^{\pm} v|_{m,K} \leq C h_K^{\min\{s+1,k\}+1-m} \|v\|_{s+2,K}, \tag{3.8}$$

$$\|v - \Pi^{\pm} v\|_{0,e} \leq C h_K^{\min\{s+1,k\}+\frac{1}{2}} \|v\|_{s+2,K} \qquad \forall e \subset \partial K, \tag{3.9}$$

$$|\boldsymbol{r} - \boldsymbol{\Pi}^{\pm} \boldsymbol{r}|_{m,K} \leq C h_K^{\min\{s,k\}+1-m} \|\boldsymbol{r}\|_{s+1,K}, \tag{3.10}$$

$$\|\boldsymbol{r} - \boldsymbol{\Pi}^{\pm} \boldsymbol{r}\|_{0,e} \leq C h_K^{\min\{s,k\}+\frac{1}{2}} \|\boldsymbol{r}\|_{s+1,K} \qquad \forall e \subset \partial K. \tag{3.11}$$

*Furthermore, for any edge $e_i$ parallel to the $x_i$-axis, $i = 1, 2$, we have*

$$\|w - \pi_i^{\pm} w\|_{0,e_i} \leq C h_{e_i}^{\min\{s+\frac{1}{2},k\}+1} \|w\|_{s+\frac{3}{2},e_i} \qquad \forall w \in H^{s+\frac{3}{2}}(e_i) \tag{3.12}$$

*with $h_{e_i}$ denoting the length of $e_i$. Finally, if $v \in W^{s+1,\infty}(K)$, then*

$$\|v - \Pi^{\pm} v\|_{L^\infty(e)} \le C\, h_K^{\min\{s,k\}+1} \|v\|_{W^{s+1,\infty}(K)} \qquad \forall e \subset \partial K. \tag{3.13}$$

*The constant $C$ depends solely on $s$, $k$, and $\sigma$.*

*Proof.* The one-dimensional estimate (3.12) for $\pi_i^{\pm}$ has been proven in [4, 9]. Since $\Pi^{\pm}$ and $\mathbf{\Pi}^{\pm}$ are linear and polynomial preserving operators, the remaining estimates follow from the Bramble–Hilbert lemma and standard scaling arguments. For the sake of completeness, we give the detailed proof.

We begin by proving (3.10) and (3.11). Consider $\widehat{K} = (-1,1)^2$, and set $t := \min\{s,k\}$. For $\boldsymbol{q} \in \mathcal{Q}^k(\widehat{K})^2$, we define $|||\boldsymbol{q}|||_{\pm}^2 := \|\boldsymbol{q}_0\|_{0,\widehat{K}}^2 + \|\boldsymbol{q}_\perp \cdot \boldsymbol{n}_{\widehat{K}}\|_{\widehat{\gamma}_1^{\pm}}^2 + \|\boldsymbol{q}_\perp \cdot \boldsymbol{n}_{\widehat{K}}\|_{\widehat{\gamma}_2^{\pm}}^2$, where $\boldsymbol{q}_0$ is the $L^2$-projection of $\boldsymbol{q}$ onto the subspace $\nabla \mathcal{Q}^k(\widehat{K})$ of $\mathcal{Q}^k(\widehat{K})^2$, and $\boldsymbol{q}_\perp$ is the $L^2$-orthogonal complement. It can be seen that $|||\cdot|||_{\pm}$ is a norm in $\mathcal{Q}^k(\widehat{K})^2$. If now $\boldsymbol{r} \in H^{t+1}(\widehat{K})^2$, from the norm equivalence in finite dimensional spaces, conditions (3.4), (3.5), and the trace theorem, we have $\|\mathbf{\Pi}^{\pm}\boldsymbol{r}\|_{m,\widehat{K}} \le C|||\mathbf{\Pi}^{\pm}\boldsymbol{r}|||_{\pm} \le C\|\boldsymbol{r}\|_{1,\widehat{K}}$, and therefore $\|\mathbf{\Pi}^{\pm}\boldsymbol{r}\|_{m,\widehat{K}} \le C\|\boldsymbol{r}\|_{t+1,\widehat{K}}$. The identity operator is also continuous from $H^{t+1}(\widehat{K})^2$ into $H^m(\widehat{K})^2$, and hence $\|\boldsymbol{r} - \mathbf{\Pi}^{\pm}\boldsymbol{r}\|_{m,\widehat{K}} \le C\|\boldsymbol{r}\|_{t+1,\widehat{K}}$. Since $\boldsymbol{r} - \mathbf{\Pi}^{\pm}\boldsymbol{r} = \mathbf{0}$ for all polynomials $\boldsymbol{r}$ of degree $\le t$ in each variable, we can apply the classical Bramble–Hilbert lemma (cf., e.g., [5, Theorem 3.1.1]) and replace the full $H^{t+1}$-norm by the $H^{t+1}$-seminorm:

$$\|\boldsymbol{r} - \mathbf{\Pi}^{\pm}\boldsymbol{r}\|_{m,\widehat{K}} \le C|\boldsymbol{r}|_{t+1,\widehat{K}}, \quad m = 0, 1.$$

Furthermore, by the trace theorem we have $\|\boldsymbol{r} - \mathbf{\Pi}^{\pm}\boldsymbol{r}\|_{0,\partial\widehat{K}} \le C\|\boldsymbol{r} - \mathbf{\Pi}^{\pm}\boldsymbol{r}\|_{1,\widehat{K}}$, and thus

$$\|\boldsymbol{r} - \mathbf{\Pi}^{\pm}\boldsymbol{r}\|_{0,\partial\widehat{K}} \le C|\boldsymbol{r}|_{t+1,\widehat{K}}.$$

The estimates (3.10) and (3.11) on a general element $K$ can now be obtained by scaling arguments.

The estimates (3.8), (3.9), and (3.13) can be proven as follows. Lemma 3.7 in [9] states that the one-dimensional operators $\pi_i^{\pm}$ satisfy $\|\pi_i^{\pm} v\|_{0,\widehat{I}}^2 \le C\|v\|_{0,\widehat{I}}^2 + C|v(\pm 1)|^2$ with $\widehat{I} = (-1,1)$. From this continuity property, recalling the definition (3.3), we obtain $\|\Pi^{\pm} v\|_{0,\widehat{K}} \le C\|v\|_{C^0(\overline{\widehat{K}})}$, and since $H^2(\widehat{K})$ is continuously embedded into $C^0(\overline{\widehat{K}})$ [5, p. 114], we have $\|\Pi^{\pm} v\|_{0,\widehat{K}} \le C\|v\|_{2,\widehat{K}}$. As before, from the norm equivalence in finite dimensional spaces, the continuity of the identity operator from $H^{t+1}(\widehat{K})$ into $H^m(\widehat{K})$, and the Bramble–Hilbert lemma, we conclude that, for $m = 0, 1$,

$$\|v - \Pi^{\pm} v\|_{m,\widehat{K}} \le C \begin{cases} |v|_{\min\{s+1,k\}+1,\widehat{K}} & \text{if } k \ge 1, \\ |v|_{1,\widehat{K}} + |v|_{2,\widehat{K}} & \text{if } k = 0, \end{cases}$$

as well as

$$\|v - \Pi^{\pm} v\|_{0,\partial\widehat{K}} \le C \begin{cases} |v|_{\min\{s+1,k\}+1,\widehat{K}} & \text{if } k \ge 1, \\ |v|_{1,\widehat{K}} + |v|_{2,\widehat{K}} & \text{if } k = 0. \end{cases}$$

The estimates (3.8) and (3.9) then follow from scaling arguments. Finally, (3.13) can be proven similarly by using the continuous embedding of $W^{1,\infty}(\widehat{K})$ into $C^0(\overline{\widehat{K}})$. ∎

**3.3. The functionals $K_{\mathcal{A}}$ and $K_{\mathcal{B}}$.** In this subsection, we obtain the functionals $K_{\mathcal{A}}$ and $K_{\mathcal{B}}$ introduced in subsection 3.1, corresponding to the projections $\mathbf{\Pi}$ and $\Pi$ in (3.7). We consider the stabilization parameter $C_{11}$ defined by (2.15), in order to highlight the fact that any choice of $\alpha \neq 0$ in (2.15) deteriorates the rates of convergence of the estimates of Theorem 2.1.

In [3, Corollary 3.4], $K_{\mathcal{A}}$ has been investigated for general projection operators $\mathbf{\Pi}$ and $\Pi$ satisfying the approximation results in Lemma 3.2. Thus, we just report the final result here.

LEMMA 3.3 (cf. [3]). *Let $u \in H^{s+2}(\Omega)$, $s \geq 0$, and $\varphi \in H^{t+2}(\Omega)$ , $t \geq 0$. Assume $C_{11}$ to be given by* (2.15). *Then, if we set $\boldsymbol{q} = \nabla u$ and $\mathbf{\Phi} = \pm\nabla\varphi$, the approximation property* (3.1) *holds true with*

$$K_{\mathcal{A}}(\boldsymbol{q}, u; \mathbf{\Phi}, \varphi) = C\big[h^{\min\{s,k\}+1}(h^{\min\{t,k\}+1} + h^{\min\{t+1,k\}}) + h^{\min\{s+1,k\}+1}(h^{\min\{t,k\}} + \zeta h^{\min\{t+1,k\}+\alpha})\big]\|u\|_{s+2}\|\varphi\|_{t+2}.$$

*Furthermore, in the particular case where $(\mathbf{\Phi}, \varphi) = (\boldsymbol{q}, u)$, there holds*

$$K_{\mathcal{A}}(\boldsymbol{q}, u; \boldsymbol{q}, u) = C\big[h^{2\min\{s,k\}+2} + \zeta h^{2\min\{s+1,k\}+1+\alpha}\big]\|u\|^2_{s+2}.$$

*The constant $C$ depends solely on $s$, $t$, $k$, and $\sigma$.*

In [3], the functional $K_{\mathcal{B}}$ was studied only in the case where $\mathbf{\Pi}$ and $\Pi$ are $\mathrm{L}^2$-projections. Next, we show that a better result for $K_{\mathcal{B}}$ can be obtained on Cartesian grids for the projections defined by (3.7) and the numerical fluxes defined by (2.11). To obtain this result, we use the following inverse inequality, which easily follows from standard scaling arguments.

LEMMA 3.4. *There exists a positive constant $C$ depending solely on $k$ and $\sigma$ such that $\forall \boldsymbol{s} \in \boldsymbol{M}_N$ we have*

$$\|\boldsymbol{s}\|_{0,e} \leq C h_K^{-\frac{1}{2}} \|\boldsymbol{s}\|_{0,K}$$

*$\forall K \in \mathcal{T}$, $e$ being any side of $K$.*

We set $u_\Gamma = u|_\Gamma$, and $\|u_\Gamma\|^2_{s+\frac{3}{2},\Gamma} = \sum_{j=1}^4 \|u_\Gamma\|^2_{s+\frac{3}{2},\Gamma_j}$, where $\{\Gamma_j\}_{j=1}^4$ denote the sides of $\Gamma$. We are now ready to state our main lemma.

LEMMA 3.5. *Let $u \in H^{s+2}(\Omega)$, $s \geq 0$, and set $\boldsymbol{q} = \nabla u$. Assume further that $u \in W^{s+1,\infty}(E_{\mathcal{N}})$ if $\Gamma_{\mathcal{N}} \cap \Gamma^- \neq \emptyset$. Assume $C_{11}$ to be given by* (2.15) *, and let $\mathbf{\Pi}$ and $\Pi$ be the operators defined by* (3.7). *Then, for any $(\boldsymbol{r}, w) \in \boldsymbol{M}_N \times V_N$, the approximation property* (3.2) *holds true, with $K_{\mathcal{B}}$ given by*

$$K_{\mathcal{B}}(\boldsymbol{q}, u) := C\,[h^{\min\{s,k\}+1} + \zeta^{-\frac{1}{2}} h^{\min\{s,k\}+\frac{1}{2}-\frac{\alpha}{2}} + \zeta^{\frac{1}{2}} h^{\min\{s+1,k\}+\frac{1}{2}+\frac{\alpha}{2}}]\|u\|_{s+2} + C\,|\,\Gamma_{\mathcal{N}} \cap \Gamma^-\,|^{\frac{1}{2}}\, h^{\min\{s,k\}+\frac{1}{2}}\|\,u\,\|_{W^{s+1,\infty}(E_{\mathcal{N}})} + C\,h^{\min\{s+\frac{1}{2},k\}+\frac{1}{2}}\|u_\Gamma\|_{s+\frac{3}{2},\Gamma},$$

*where the constant $C$ depends solely on $s$, $k$, and $\sigma$, and where $|\,\Gamma_{\mathcal{N}} \cap \Gamma^-\,|$ denotes the $(d-1)$–dimensional measure of $\Gamma_{\mathcal{N}} \cap \Gamma^-$.*

*Proof.* In order to be able to distinguish the many parts of $\Gamma$ and facilitate the proof of the above result, we introduce the following notation:

$$\begin{aligned}
&\mathcal{E}^+ := \{e \subset \Gamma :\ \boldsymbol{v}\cdot\boldsymbol{n} > 0\}, && \mathcal{E}^- := \{e \subset \Gamma :\ \boldsymbol{v}\cdot\boldsymbol{n} < 0\},\\
&\mathcal{E}_1^+ := \{e \in \mathcal{E}^+|\ x_2 = \text{const}\}, && \mathcal{E}_1^- := \{e \in \mathcal{E}^-|\ x_2 = \text{const}\},\\
&\mathcal{E}_2^+ := \{e \in \mathcal{E}^+|\ x_1 = \text{const}\}, && \mathcal{E}_2^- := \{e \in \mathcal{E}^-|\ x_1 = \text{const}\},
\end{aligned}$$

and we define $\mathcal{E}_i := \mathcal{E}_i^+ \cup \mathcal{E}_i^-$; these boundaries are indicated in Figure 3.1.

We set $\boldsymbol{\xi_q} := \boldsymbol{q} - \boldsymbol{\Pi q}$ and $\xi_u := u - \Pi u$, write

$$|\mathcal{A}(\boldsymbol{r}, v; \boldsymbol{\xi_q}, \xi_u)| \le |a(\boldsymbol{r}, \boldsymbol{\xi_q})| + |b(v, \boldsymbol{\xi_q})| + |b(\xi_u, \boldsymbol{r})| + |c(\xi_u, v)| =: T_1 + T_2 + T_3 + T_4,$$

and estimate each of the forms separately.

a. Estimate of $T_1$. From Lemma 3.2, we have

$$T_1 = \left| \sum_{K\in\mathcal{T}} \int_K \boldsymbol{r}\cdot\boldsymbol{\xi_q}\, d\boldsymbol{x} \right| \le \left( \sum_{K\in\mathcal{T}} \|\boldsymbol{r}\|_{0,K}^2 \right)^{\frac12} \left( \sum_{K\in\mathcal{T}} \|\boldsymbol{\xi_q}\|_{0,K}^2 \right)^{\frac12}$$
$$\le C |\,(\boldsymbol{r}, v)\,|_{\mathcal{A}} \left( \sum_{K\in\mathcal{T}} h_K^{2\min\{s,k\}+2} \|\boldsymbol{q}\|_{s+1,K}^2 \right)^{\frac12}.$$

b. Estimate of $T_2$. We can write

$$T_2 = \Bigg| - \sum_{K\in\mathcal{T}} \int_K \nabla v\cdot\boldsymbol{\xi_q}\, d\boldsymbol{x}$$
$$+ \sum_{e\in\mathcal{E}_\mathcal{I}} \int_e [\![v]\!]\cdot(\{\!\{\boldsymbol{\xi_q}\}\!\} - \boldsymbol{C}_{12}[\![\boldsymbol{\xi_q}]\!])\, ds + \sum_{e\in\mathcal{E}_\mathcal{D}} \int_e v\,\boldsymbol{\xi_q}\cdot\boldsymbol{n}\, ds \Bigg|.$$

Taking into account the definition of the fluxes in (2.11) and of the projection $\boldsymbol{\Pi}$ in (3.4) and (3.5), we conclude that

$$\int_K \nabla v\cdot\boldsymbol{\xi_q}\, d\boldsymbol{x} = 0 \quad \forall K\in\mathcal{T}, \qquad \int_e v\,\boldsymbol{\xi_q}\cdot\boldsymbol{n}\, ds = 0 \quad \forall e\in\mathcal{E}^-,$$
$$\int_e [\![v]\!]\cdot(\{\!\{\boldsymbol{\xi_q}\}\!\} - \boldsymbol{C}_{12}[\![\boldsymbol{\xi_q}]\!])\, ds = 0 \quad \forall e\in\mathcal{E}_\mathcal{I}.$$

Consequently,

$$T_2 = \left| \sum_{e\in\mathcal{E}^+\cap\mathcal{E}_\mathcal{D}} \int_e v\,\boldsymbol{\xi_q}\cdot\boldsymbol{n}\, ds \right|.$$

Multiplying and dividing each term of the sum by $C_{11}^{\frac12}$, and using the approximation properties of $\boldsymbol{\Pi}$ in Lemma 3.2, we have

$$T_2 = \left| \sum_{e\in\mathcal{E}^+\cap\mathcal{E}_\mathcal{D}} \int_e v\,\boldsymbol{\xi_q}\cdot\boldsymbol{n}\, ds \right| \le \left( \sum_{e\in\mathcal{E}^+\cap\mathcal{E}_\mathcal{D}} C_{11}\|v\|_{0,e}^2 \right)^{\frac12} \left( \sum_{e\in\mathcal{E}^+\cap\mathcal{E}_\mathcal{D}} C_{11}^{-1}\|\boldsymbol{\xi_q}\|_{0,e}^2 \right)^{\frac12}$$
$$\le C\,|\,(\boldsymbol{r}, v)\,|_{\mathcal{A}} \left( \zeta^{-1} \sum_{e\in\mathcal{E}^+\cap\mathcal{E}_\mathcal{D}} h_{K_e}^{2\min\{s,k\}+1-\alpha} \|\boldsymbol{q}\|_{s+1,K_e}^2 \right)^{\frac12}.$$

Note that we have used the shape-regularity assumption (2.12) to bound $C_{11}^{-1}$ by $C\,\zeta^{-1} h_{K_e}^{-\alpha}$.

c. Estimate of $T_4$. We have

$$\begin{aligned}
T_4 &= \left| \sum_{e\in\mathcal{E}_\mathcal{I}} \int_e C_{11}[\![v]\!]\cdot[\![\xi_u]\!]\,ds + \sum_{e\in\mathcal{E}_\mathcal{D}} \int_e C_{11} v\,\xi_u\,ds \right| \\
&\le \left( \sum_{e\in\mathcal{E}_\mathcal{I}} C_{11}\|[\![v]\!]\|_{0,e}^2 + \sum_{e\in\mathcal{E}_\mathcal{D}} C_{11}\|v\|_{0,e}^2 \right)^{\frac12} \cdot \left( \sum_{e\in\mathcal{E}_\mathcal{I}} C_{11}\|[\![\xi_u]\!]\|_{0,e}^2 + \sum_{e\in\mathcal{E}_\mathcal{D}} C_{11}\|\xi_u\|_{0,e}^2 \right)^{\frac12} \\
&\le C|(\boldsymbol{r},v)|_\mathcal{A} \left( \sum_{K\in\mathcal{T}} \sum_{e\subset\partial K} C_{11}\|\xi_u\|_{0,e}^2 \right)^{\frac12} \\
&\le C|(\boldsymbol{r},v)|_\mathcal{A} \left( \zeta \sum_{K\in\mathcal{T}} h_K^{2\min\{s+1,k\}+1+\alpha}\|u\|_{s+2,K}^2 \right)^{\frac12} \\
&\le C\,|(\boldsymbol{r},v)|_\mathcal{A} \left( \zeta h^{2\min\{s+1,k\}+1+\alpha}\|u\|_{s+2}^2 \right)^{\frac12}.
\end{aligned}$$

d. Estimate of $T_3$. This estimate cannot be obtained as easily as the previous ones since it is here that the key idea introduced by LeSaint and Raviart [8] has to be suitably applied. We start by writing

$$\begin{aligned}
T_3 &= \left| \sum_{K\in\mathcal{T}} \int_K \xi_u\,\nabla\cdot\boldsymbol{r}\,d\boldsymbol{x} - \sum_{e\in\mathcal{E}_\mathcal{I}} \int_e (\{\!\{\xi_u\}\!\} + \boldsymbol{C}_{12}\cdot[\![\xi_u]\!])[\![\boldsymbol{r}]\!]\,ds - \sum_{e\in\mathcal{E}_\mathcal{N}} \int_e \xi_u\,\boldsymbol{r}\cdot\boldsymbol{n}\,ds \right| \\
&= \left| \sum_{K\in\mathcal{T}} \int_K \xi_u\,\nabla\cdot\boldsymbol{r}\,d\boldsymbol{x} - \sum_{K\in\mathcal{T}} \left( \sum_{\substack{e\subset\partial K \\ e\in\mathcal{E}_\mathcal{I}}} \int_e (\{\!\{\xi_u\}\!\} + \boldsymbol{C}_{12}\cdot[\![\xi_u]\!])\boldsymbol{r}\cdot\boldsymbol{n}_{\boldsymbol{K}}\,ds \right) \right. \\
&\quad \left. - \sum_{e\in\mathcal{E}_\mathcal{N}} \int_e \xi_u\,\boldsymbol{r}\cdot\boldsymbol{n}\,ds \right|.
\end{aligned}$$

Again with (2.11) and the notation in Figure 3.1, we see that the contribution of an interior element $K$ to this expression is

$$Z_K(\boldsymbol{r},u) := \int_K \xi_u\,\nabla\cdot\boldsymbol{r}\,d\boldsymbol{x} - \int_{\gamma_1^+\cup\gamma_2^+} \xi_u\boldsymbol{r}\cdot\boldsymbol{n}_{\boldsymbol{K}}\,ds - \int_{\gamma_1^-\cup\gamma_2^-} \xi_u^{\text{out}}\boldsymbol{r}\cdot\boldsymbol{n}_{\boldsymbol{K}}\,ds,$$

where the superscript "out" denotes the traces taken from outside $K$. Since $u^{\text{out}}_{|_{\gamma_i^\pm}} = u_{|_{\gamma_i^\pm}}$ and $[\Pi u]^{\text{out}}_{|_{\gamma_i^-}} = \pi_i^+(u_{|_{\gamma_i^-}})$ for the corresponding one-dimensional projection $\pi_i^+$, this contribution can be written as

$$\begin{aligned}
Z_K(\boldsymbol{r},u) &= \int_K (u-\Pi^+u)\,\nabla\cdot\boldsymbol{r}\,d\boldsymbol{x} - \int_{\gamma_1^+} (u-\pi_1^+u)\,\boldsymbol{r}\cdot\boldsymbol{n}_{\boldsymbol{K}}\,ds \\
&\quad - \int_{\gamma_2^+} (u-\pi_2^+u)\,\boldsymbol{r}\cdot\boldsymbol{n}_{\boldsymbol{K}}\,ds - \int_{\gamma_1^-} (u-\pi_1^+u)\boldsymbol{r}\cdot\boldsymbol{n}_{\boldsymbol{K}}\,ds - \int_{\gamma_2^-} (u-\pi_2^+u)\boldsymbol{r}\cdot\boldsymbol{n}_{\boldsymbol{K}}\,ds.
\end{aligned} \tag{3.14}$$

For boundary elements, we add and subtract corresponding terms to obtain

$$\begin{aligned} T_3 &\le \left| \sum_{K\in\mathcal{T}} Z_K(\boldsymbol{r},u) \right| + \left| \sum_{e\in\mathcal{E}_1} \int_e (u_\Gamma - \pi_1^+ u_\Gamma)\, \boldsymbol{r}\cdot\boldsymbol{n}\, ds \right. \\ &\qquad \left. + \sum_{e\in\mathcal{E}_2} \int_e (u_\Gamma - \pi_2^+ u_\Gamma)\, \boldsymbol{r}\cdot\boldsymbol{n}\, ds + \sum_{e\in\mathcal{E}_\mathcal{N}} \int_e \xi_u \boldsymbol{r}\cdot\boldsymbol{n}\, ds \right| \\ &\le \sum_{K\in\mathcal{T}} |Z_K(\boldsymbol{r},u)| + \sum_{e\in\mathcal{E}_1\setminus(\mathcal{E}_\mathcal{N}\cap\mathcal{E}^-)} \int_e |(u_\Gamma - \pi_1^+ u_\Gamma)\, \boldsymbol{r}\cdot\boldsymbol{n}|\, ds \\ &\quad + \sum_{e\in\mathcal{E}_2\setminus(\mathcal{E}_\mathcal{N}\cap\mathcal{E}^-)} \int_e |(u_\Gamma - \pi_1^+ u_\Gamma)\, \boldsymbol{r}\cdot\boldsymbol{n}|\, ds + \sum_{e\in\mathcal{E}_\mathcal{N}\cap\mathcal{E}^-} \int_e |\xi_u\, \boldsymbol{r}\cdot\boldsymbol{n}\,| ds, \end{aligned}$$

with $Z_K(\boldsymbol{r},u)$ defined in (3.14).

We start by bounding the contributions to $T_3$ stemming from a boundary edge $e_i \in \mathcal{E}_i \setminus (\mathcal{E}_\mathcal{N}\cap\mathcal{E}^-)$ parallel to the $x_i$-axis, $i=1,2$. Since $u\in H^{s+2}(\Omega)$ implies $u_\Gamma \in H^{s+\frac{3}{2}}(e_i)$, by Lemma 3.2 and the inverse inequality in Lemma 3.4, we get

$$\begin{aligned} \int_{e_i} |(u_\Gamma - \pi_i^\pm u_\Gamma)\, \boldsymbol{r}\cdot\boldsymbol{n}|\, ds &\le \|u_\Gamma - \pi_i^\pm u_\Gamma\|_{0,e_i}\, \|\boldsymbol{r}\|_{0,e_i} \\ &\le C h_{K_{e_i}}^{\min\{s+\frac{1}{2},k\}+\frac{1}{2}} \|u_\Gamma\|_{s+\frac{3}{2},e_i}\, \|\boldsymbol{r}\|_{0,K_{e_i}}. \end{aligned}$$

Here, $K_{e_i}$ denotes again the element containing the edge $e_i$. Consequently, the global contribution to $T_3$ of the boundary edges belonging to $\mathcal{E}_i \setminus (\mathcal{E}_\mathcal{N}\cap\mathcal{E}^-)$ can be bounded by

$$\begin{aligned} &\sum_{e\in(\mathcal{E}_1\cup\mathcal{E}_2)\setminus(\mathcal{E}_\mathcal{N}\cap\mathcal{E}^-)} C h_{K_e}^{\min\{s+\frac{1}{2},k\}+\frac{1}{2}} \|u_\Gamma\|_{s+\frac{3}{2},e}\, \|\boldsymbol{r}\|_{0,K_e} \\ &\quad \le C \left( \sum_{e\subset\Gamma} h_{K_e}^{2\min\{s+\frac{1}{2},k\}+1} \|u_\Gamma\|_{s+\frac{3}{2},e}^2 \right)^{\frac{1}{2}} \left( \sum_{e\subset\Gamma} \|\boldsymbol{r}\|_{0,K_e}^2 \right)^{\frac{1}{2}} \\ &\quad \le C h^{\min\{s+\frac{1}{2},k\}+\frac{1}{2}} \left( \sum_{e\subset\Gamma} \|u_\Gamma\|_{s+\frac{3}{2},e}^2 \right)^{\frac{1}{2}} |\,(\boldsymbol{r},v)\,|_\mathcal{A} \\ &\quad \le C h^{\min\{s+\frac{1}{2},k\}+\frac{1}{2}} \|u_\Gamma\|_{s+\frac{3}{2},\Gamma}\, |\,(\boldsymbol{r},v)\,|_\mathcal{A}. \end{aligned}$$

For the edges $e$ in $\mathcal{E}_\mathcal{N}\cap\mathcal{E}^-$, we have to use a different argument. Thus, by Lemma 3.4, we have

$$\begin{aligned} \int_e |\xi_u\, \boldsymbol{r}\cdot\boldsymbol{n}|\, ds &\le \|\,\xi_u\,\|_{L^\infty(e)}\, \|\,\boldsymbol{r}\cdot\boldsymbol{n}\,\|_{L^1(e)} \\ &\le C\,|e|^{\frac{1}{2}}\, h_{K_e}^{-\frac{1}{2}}\, \|\,\xi_u\,\|_{L^\infty(e)}\, \|\,\boldsymbol{r}\,\|_{0,K_e}. \end{aligned}$$

Hence, by the Cauchy–Schwarz inequality,

$$\sum_{e\in\mathcal{E}_\mathcal{N}\cap\mathcal{E}^-} \int_e |\xi_u\, \boldsymbol{r}\cdot\boldsymbol{n}\,| ds \le C\,|\,\Gamma_\mathcal{N}\cap\Gamma^-\,|^{\frac{1}{2}} \left( \sup_{e\in\mathcal{E}_\mathcal{N}\cap\mathcal{E}^-} h_{K_e}^{-\frac{1}{2}}\, \|\,\xi_u\,\|_{L^\infty(e)} \right) \|\,\boldsymbol{r}\,\|_0,$$

and so

$$\sum_{e\in\mathcal{E}_{\mathcal{N}}\cap\mathcal{E}^-}\int_e |\xi_u\,\boldsymbol{r}\cdot\boldsymbol{n}\,|ds \le C\,|\,\Gamma_{\mathcal{N}}\cap\Gamma^-\,|^{\frac12}\,h^{\min\{s,k\}+\frac12}\|\,u\,\|_{W^{s+1,\infty}(E_{\mathcal{N}})}\,|(\boldsymbol{r},v)|_{\mathcal{A}}.$$

Finally, we estimate $Z_K(\boldsymbol{r},u)$ by using the following superconvergence result, essentially due to LeSaint and Raviart [8], whose proof is postponed to subsection 3.4.

LEMMA 3.6. *Let $Z_K(\boldsymbol{r},u)$ be defined by* (3.14). *Then we have for $s\ge 0$*

$$|Z_K(\boldsymbol{r},u)| \le C\,h_K^{\min\{s,k\}+1}\|u\|_{s+2,K}\,\|\boldsymbol{r}\|_{0,K}.$$

*The constant $C$ depends only on $s$, $k$, and $\sigma$.*

By combining the result of Lemma 3.6 with the above estimates of the contribution of boundary edges, we obtain

$$\begin{aligned}T_3 \le C\,|(\boldsymbol{r},v)|_{\mathcal{A}}\Big(&h^{\min\{s,k\}+1}\,\|u\|_{s+2}+h^{\min\{s+\frac12,k\}+\frac12}\|u_\Gamma\|_{s+\frac32,\Gamma}\\&+|\,\Gamma_{\mathcal{N}}\cap\Gamma^-\,|^{\frac12}\,h^{\min\{s,k\}+\frac12}\|\,u\,\|_{W^{s+1,\infty}(E_{\mathcal{N}})}\Big).\end{aligned}$$

*Conclusion.* The result in Lemma 3.5 now follows by simply gathering the estimates for $T_i$, $i=1,2,3,4$, obtained above. This completes the proof. ∎

**3.4. Proof of Lemma 3.6.** Writing $\boldsymbol{r}=(r_1,r_2)$, we have

$$Z_K(\boldsymbol{r},u)=Z_{K,1}(r_1,u)+Z_{K,2}(r_2,u),$$

where

$$\begin{aligned}Z_{K,1}(r_1,u)=&\int_K(u-\Pi^+u)\frac{\partial r_1}{\partial x_1}\,dx_1dx_2-\int_{\gamma_2^+}(u-\pi_2^+u)\,r_1\,dx_2\\&+\int_{\gamma_2^-}(u-\pi_2^+u)\,r_1\,dx_2\end{aligned}$$

and

$$\begin{aligned}Z_{K,2}(r_2,u)=&\int_K(u-\Pi^+u)\frac{\partial r_2}{\partial x_2}\,dx_1dx_2-\int_{\gamma_1^+}(u-\pi_1^+u)\,r_2\,dx_1\\&+\int_{\gamma_1^-}(u-\pi_1^+u)\,r_2\,dx_1.\end{aligned}$$

The proof of the approximation results for $Z_{K,1}$ and $Z_{K,2}$ are analogous; therefore, we just present the one for $Z_{K,1}$, essentially following the same arguments as in [8].

First, we consider $Z_{K,1}$ on the reference square $(-1,1)^2$. We claim that

$$Z_{K,1}(r_1,u)=0\qquad\forall u\in\mathcal{P}^{k+1}(K),\quad r_1\in\mathcal{Q}^k(K). \tag{3.15}$$

To prove (3.15), fix $r_1\in\mathcal{Q}^k(K)$. Since $\Pi^+$ and $\pi^+$ are polynomial preserving operators, (3.15) holds true for every $u\in\mathcal{Q}^k(K)$. Therefore, we just have to consider the cases $u(x_1,x_2)=x_1^{k+1}$ and $u(x_1,x_2)=x_2^{k+1}$.

Let us start with $u(x_1,x_2)=x_1^{k+1}$. On $\gamma_2^+$ we have $u=\pi_2^+u=1$, and on $\gamma_2^-$ we have $u=\pi_2^+u=(-1)^{k+1}$. Since $\frac{\partial r_1}{\partial x_1}$ is a polynomial of degree at most $k-1$ in $x_1$, we obtain

$$\int_K(u-\Pi^+u)\frac{\partial r_1}{\partial x_1}\,dx_1dx_2=\int_K(u-\pi_1^+u)\frac{\partial r_1}{\partial x_1}\,dx_1dx_2=0.$$

Thus, $Z_{K,1}(r_1,u)=0$ for $u(x_1,x_2)=x_1^{k+1}$.

In the case $u(x_1,x_2)=x_2^{k+1}$, we integrate by parts and obtain

$$\int_K (u-\Pi^+u)\frac{\partial r_1}{\partial x_1}\,dx_1dx_2 = -\int_K \frac{\partial(u-\Pi^+u)}{\partial x_1} r_1\,dx_1dx_2 + \int_{\gamma_2^+}(u-\pi_2^+u)r_1\,dx_1 - \int_{\gamma_2^-}(u-\Pi^+u)r_1\,dx_2.$$

Since $\frac{\partial(u-\Pi^+u)}{\partial x_1}=0$ and $\Pi^+u_{|_{\gamma_2^-}}=\pi_2^+u_{|_{\gamma_2^-}}$ due to the special form of $u$, we conclude that $Z_{K,1}(r_1,u)=0$ also for $u(x_1,x_2)=x_2^{k+1}$. This completes the proof of (3.15).

For fixed $r_1\in\mathcal{Q}^k(K)$, the linear functional $u\mapsto Z_{K,1}(r_1,u)$ is continuous on $H^{s+2}(K)$ with norm bounded by $C\|r_1\|_{0,K}$. Due to (3.15), it vanishes over $\mathcal{P}^{s+1}(K)$ for $0\le s\le k$. Hence, by applying the Bramble–Hilbert lemma (see [6, Lemma 6], for instance), we obtain for $u\in H^{s+2}(K)$ that

$$|Z_{K,1}(r_1,u)|\le C|u|_{s+2,K}\|r_1\|_{0,K}.$$

This proves the assertion on the reference element $(-1,1)^2$. The general case follows from a standard scaling argument.

**3.5. Proof of Theorem 2.1.** If the exact solution of our model problem, $(\boldsymbol{q},u)$, belongs to $H^{k+1}(\Omega)^2\times H^{k+2}(\Omega)$, with $k\ge 0$, and if $u\in W^{k+1,\infty}(E_{\mathcal{N}})$ in the case where $\Gamma_{\mathcal{N}}\cap\Gamma^-\neq\emptyset$, Lemmas 3.3 and 3.5 give

$$K_{\mathcal{A}}(\boldsymbol{q},u;\boldsymbol{q},u)\le Ch^{2k+1+\alpha}\|u\|_{k+2}^2,$$

and

$$K_{\mathcal{B}}(\boldsymbol{q},u)\le Ch^{k+\frac12-\frac{|\alpha|}{2}}\|u\|_{k+2}+Ch^{k+\frac12}\|u_\Gamma\|_{k+\frac32,\Gamma} + C|\,\Gamma_{\mathcal{N}}\cap\Gamma^-\,|^{\frac12}\,h^{k+\frac12}\|\,u\,\|_{W^{k+1,\infty}(E_{\mathcal{N}})}$$

with $u_\Gamma=u_{|\Gamma}$. The estimate of the error $|\,(\boldsymbol{q}-\boldsymbol{q}_N,u-u_N)\,|_{\mathcal{A}}$ now follows from Lemma 3.1. Notice that $\alpha=0$ gives the best order of convergence in $h$ equal to $k+\frac12$.

Our assumptions on the domain imply that the solution $\varphi$ of the adjoint problem in Lemma 3.1 belongs to $H^2(\Omega)$ and that we have $\|\varphi\|_2\le C\|\lambda\|_0$. Hence, we conclude that

$$K_{\mathcal{A}}(\boldsymbol{q},u;\boldsymbol{\Phi},\varphi)\le C\begin{cases}h^{k+1}\|u\|_{k+2}\|\lambda\|_0, & k\ge 1,\\ h^{1+\min(0,\alpha)}\|u\|_2\|\lambda\|_0, & k=0,\end{cases}$$

$$K_{\mathcal{B}}(\Phi,\varphi)\le Ch^{\frac12-\frac{|\alpha|}{2}}\|\lambda\|_0.$$

The estimate of $\|u-u_N\|_0$ thus follows from Lemma 3.1. Notice that $\alpha=0$ gives again the best order of convergence in $h$ which is $k+1$.

**4. Numerical experiments.** In this section, we display a series of numerical experiments showing the *computed orders of convergence* of the LDG method; we show (i) that the orders given by our theoretical results are sharp, (ii) that they can deteriorate when the stabilization parameter $C_{11}$ is not of order one, (iii) that the exact capture of the boundary conditions induces an unexpected increase of $\frac12$ in the order of convergence of the gradient, and (iv) that the orders of convergence are independent of the dimension.

In all experiments, we estimate the orders of convergence of the LDG method as follows. We consider successively refined Cartesian grids $\mathcal{T}_\ell$, $\ell \geq 0$, consisting of $2^{d\,\ell}$ uniform $d$-dimensional cubes with corresponding mesh size $2^{-\ell+1}$; we present results in two and three space dimensions. If $e(\mathcal{T}_\ell)$ denotes the error on the $\ell$th mesh, then the numerical order of convergence is computed as follows:

$$\frac{\log\left(\frac{e(\mathcal{T}_\ell)}{e(\mathcal{T}_{\ell-1})}\right)}{\log(0.5)}, \qquad \ell \geq 1.$$

The results have been obtained with the object-oriented C++ library `deal.II` developed by Bangerth and Kanschat [1].

TABLE 4.1
*Orders of convergence for the LDG method with $C_{11} = 1.0$: $\Gamma_{\mathcal{N}} = \emptyset$.*

| | | $u$ | | $q_1$ and $q_2$ | |
|---|---|---|---|---|---|
| Element | $\ell$ | $L^2$ | $L^\infty$ | $L^2$ | $L^\infty$ |
| $\mathcal{Q}^0$ | 1 | 0.5043 | 0.1284 | 0.7401 | 0.3036 |
| | 2 | 0.7974 | 0.3682 | 0.7257 | 0.4175 |
| | 3 | 0.9975 | 0.6029 | 0.7892 | 0.4574 |
| | 4 | 1.0095 | 0.7873 | 0.8803 | 0.1365 |
| | 5 | 0.9736 | 0.9019 | 0.9398 | 0.2937 |
| | 6 | 0.9683 | 0.9624 | 0.9724 | 0.3856 |
| $\mathcal{Q}^1$ | 1 | 1.7570 | 0.9753 | 1.5354 | 1.3116 |
| | 2 | 1.7999 | 1.3976 | 1.2669 | 0.7766 |
| | 3 | 1.8496 | 1.6995 | 1.2857 | 0.7150 |
| | 4 | 1.8941 | 1.8549 | 1.3640 | 0.8670 |
| | 5 | 1.9390 | 1.9305 | 1.4251 | 0.9422 |
| | 6 | 1.9681 | 1.8971 | 1.4610 | 0.9747 |
| $\mathcal{Q}^2$ | 1 | 2.7300 | 1.9615 | 2.3151 | 1.5921 |
| | 2 | 2.8570 | 2.5254 | 2.3071 | 1.6811 |
| | 3 | 2.8676 | 2.7695 | 2.3280 | 1.8300 |
| | 4 | 2.8999 | 2.8862 | 2.3901 | 1.8988 |
| | 5 | 2.9382 | 2.9428 | 2.4387 | 1.9392 |
| | 6 | 2.9661 | 2.8316 | 2.4678 | 1.9658 |
| $\mathcal{Q}^3$ | 1 | 3.6933 | 2.9236 | 3.1730 | 1.8719 |
| | 2 | 3.8108 | 3.5453 | 3.2270 | 2.5280 |
| | 3 | 3.8660 | 3.7719 | 3.3094 | 2.7551 |
| | 4 | 3.9120 | 3.8827 | 3.3859 | 2.8770 |
| | 5 | 3.9490 | 3.9398 | 3.4380 | 2.9415 |
| | 6 | 3.9661 | 3.8249 | 3.4676 | 2.9724 |

**4.1. The sharpness of the orders of convergence of Theorem 2.1.** We consider the two-dimensional model problem (1.1) on the square $\Omega = (-1, 1)^2$ with $f$ and boundary conditions chosen in such a way that the exact solution is given by $u(x_1, x_2) = \exp(x_1\, x_2)$. We consider two cases: In the first, we impose inhomogeneous Dirichlet boundary conditions on the whole boundary, and in the second, we also impose inhomogeneous Neumann boundary conditions on the edge $\{-1\} \times (-1, 1)$. The results are contained in Tables 4.1 and 4.2 where the numerical orders of convergence in the $L^2$- and $L^\infty$-norm in $u$ and $\boldsymbol{q} = (q_1, q_2)$ of the LDG method with $\mathcal{Q}^k$-elements for $k = 0, \ldots, 3$ are shown. We take $C_{11} = 1.0$ and the coefficients $\boldsymbol{C}_{12}$ as in (2.11) with $\boldsymbol{v} = (1, 1)$.

TABLE 4.2
*Orders of convergence of the LDG method with $C_{11} = 1.0$: $\Gamma_{\mathcal{N}} \neq \emptyset$.*

| | | $u$ | | $q_1$ | | $q_2$ | |
|---|---|---|---|---|---|---|---|
| Element | $\ell$ | $\mathrm{L}^2$ | $\mathrm{L}^\infty$ | $\mathrm{L}^2$ | $\mathrm{L}^\infty$ | $\mathrm{L}^2$ | $L^\infty$ |
| $\mathcal{Q}^0$ | 1 | 0.4279 | 0.0833 | 0.5632 | 0.1687 | 0.7419 | 0.2817 |
| | 2 | 0.7818 | 0.3935 | 0.6860 | 0.2553 | 0.7330 | 0.4255 |
| | 3 | 0.9281 | 0.6447 | 0.9021 | 0.4920 | 0.8168 | 0.5801 |
| | 4 | 0.9589 | 0.8134 | 1.0231 | 0.7055 | 0.9221 | 0.2833 |
| | 5 | 0.9687 | 0.9083 | 1.0463 | 0.8479 | 0.9793 | 0.4939 |
| | 6 | 0.9795 | 0.9555 | 1.0303 | 0.9283 | 0.9954 | 0.6270 |
| $\mathcal{Q}^1$ | 1 | 1.5640 | 0.8492 | 1.4414 | 0.8857 | 1.4867 | 1.0768 |
| | 2 | 1.7767 | 1.4022 | 1.4194 | 1.1787 | 1.3096 | 1.1126 |
| | 3 | 1.8567 | 1.6995 | 1.4695 | 1.1444 | 1.3162 | 0.7155 |
| | 4 | 1.9167 | 1.8549 | 1.5024 | 0.8670 | 1.3843 | 0.8669 |
| | 5 | 1.9559 | 1.9305 | 1.5117 | 0.9422 | 1.4379 | 0.9422 |
| | 6 | 1.9777 | 1.8971 | 1.5097 | 0.9747 | 1.4683 | 0.9746 |
| $\mathcal{Q}^2$ | 1 | 2.6095 | 1.8429 | 2.4038 | 1.8936 | 2.3275 | 1.8386 |
| | 2 | 2.8329 | 2.5220 | 2.4372 | 2.1265 | 2.3217 | 1.8231 |
| | 3 | 2.8806 | 2.7695 | 2.4719 | 1.9471 | 2.3803 | 1.8300 |
| | 4 | 2.9230 | 2.8862 | 2.4963 | 1.8988 | 2.4320 | 1.8988 |
| | 5 | 2.9563 | 2.9428 | 2.5042 | 1.9392 | 2.4631 | 1.9392 |
| | 6 | 2.9770 | 2.8316 | 2.5044 | 1.9658 | 2.4806 | 1.9658 |
| $\mathcal{Q}^3$ | 1 | 3.6125 | 2.8600 | 3.3206 | 2.7792 | 3.1634 | 2.5820 |
| | 2 | 3.8202 | 3.5475 | 3.3839 | 2.9180 | 3.2859 | 2.5593 |
| | 3 | 3.8916 | 3.7719 | 3.4665 | 2.7551 | 3.3743 | 2.7551 |
| | 4 | 3.9375 | 3.8827 | 3.4950 | 2.8770 | 3.4318 | 2.8770 |
| | 5 | 3.9664 | 3.9398 | 3.5022 | 2.9414 | 3.4643 | 2.9414 |
| | 6 | 3.9805 | 3.8264 | 3.5024 | 2.9722 | 3.4815 | 2.9721 |

TABLE 4.3
*$\mathcal{Q}^3$-elements with $C_{11} = 1.0$ and $\boldsymbol{C}_{12} = (0,0)$: $\Gamma_{\mathcal{N}} \neq \emptyset$.*

| | $u$ | | $q_1$ | | $q_2$ | |
|---|---|---|---|---|---|---|
| $\ell$ | $\mathrm{L}^2$ | $\mathrm{L}^\infty$ | $\mathrm{L}^2$ | $\mathrm{L}^\infty$ | $\mathrm{L}^2$ | $L^\infty$ |
| 1 | 3.5386 | 2.9273 | 2.8119 | 2.2386 | 3.10187 | 2.6656 |
| 2 | 3.5382 | 3.4400 | 2.8728 | 2.6760 | 2.95379 | 2.4402 |
| 3 | 3.5164 | 3.3338 | 2.9430 | 2.8623 | 2.89531 | 2.4346 |
| 4 | 3.5540 | 3.3287 | 2.9633 | 2.8890 | 2.85946 | 2.5681 |
| 5 | 3.6003 | 3.3161 | 2.9662 | 2.6764 | 2.84975 | 2.6776 |
| 6 | 3.6322 | 3.2542 | 2.9652 | 2.7514 | 2.86963 | 2.7515 |

In Table 4.1, we report the results for Dirichlet boundary conditions imposed on the whole boundary. Note that, because of the symmetry of the problem, the orders of convergence are exactly the same for $q_1$ and $q_2$. For $k = 0$, we see the *optimal* order of convergence of 1 in the $\mathrm{L}^2$-norm of the error of both $u$ and $\boldsymbol{q}$; note that Theorem 2.1 predicts an order of convergence of $\frac{1}{2}$ only for $\boldsymbol{q}$. However, for $k \geq 1$ the $\mathrm{L}^2$-rates are of order $k+1$ in $u$ and $k+\frac{1}{2}$ in $\boldsymbol{q}$, in full agreement with Theorem 2.1. The orders of convergence in the $L^\infty$-norm of the error in $u$ and $\boldsymbol{q}$ appear to be $k+1$ and $k$, respectively. The results displayed in Table 4.2 are those for the case of inhomogeneous Neumann boundary conditions on part of the boundary. We see that the orders of convergence in this case are the same as the ones in the pure Dirichlet case.

If $\boldsymbol{C}_{12}$ is not chosen as in (2.11), the orders $k+1$ and $k+\frac{1}{2}$ are not necessarily

TABLE 4.4
*Orders of convergence of the LDG method with $\mathcal{Q}^1$-elements.*

| | | $u$ | | $q_1$ and $q_2$ | |
|---|---|---|---|---|---|
| $C_{11}$ | $\ell$ | $L^2$ | $L^\infty$ | $L^2$ | $L^\infty$ |
| $1/h$ | 5 | 1.9607 | 1.9550 | 1.1409 | 0.8816 |
| | 6 | 1.9792 | 1.9057 | 1.1019 | 0.9366 |
| $1/h$ on $\mathcal{E}^+$ | 5 | 1.9331 | 1.7799 | 1.4240 | 0.8619 |
| 1.0 elsewhere | 6 | 1.9646 | 1.7914 | 1.4605 | 0.9268 |
| h | 5 | 1.8916 | 1.8810 | 1.4167 | 0.9405 |
| | 6 | 1.8603 | 1.7887 | 1.4564 | 0.9701 |
| $1/h$ on $\mathcal{E}^+$ | 5 | 1.8837 | 1.8810 | 1.4157 | 0.8698 |
| $h$ elsewhere | 6 | 1.8563 | 1.7887 | 1.4556 | 0.9319 |

TABLE 4.5
*Orders of convergence of the LDG method with $\mathcal{Q}^2$-elements.*

| | | $u$ | | $q_1$ and $q_2$ | |
|---|---|---|---|---|---|
| $C_{11}$ | $\ell$ | $L^2$ | $L^\infty$ | $L^2$ | $L^\infty$ |
| $1/h$ | 5 | 2.9555 | 2.9541 | 2.2223 | 1.8475 |
| | 6 | 2.9754 | 2.9584 | 2.1685 | 1.9228 |
| $1/h$ on $\mathcal{E}^+$ | 5 | 2.9340 | 2.8836 | 2.4358 | 1.8828 |
| 1.0 elsewhere | 6 | 2.9634 | 2.7424 | 2.4663 | 1.9427 |
| h | 5 | 2.8559 | 2.9524 | 2.4350 | 1.9483 |
| | 6 | 2.8240 | 2.5482 | 2.4656 | 1.9742 |
| $1/h$ on $\mathcal{E}^+$ | 5 | 2.8505 | 2.8642 | 2.4325 | 1.8760 |
| $h$ elsewhere | 6 | 2.8211 | 2.4554 | 2.4643 | 1.9365 |

obtained. This is demonstrated in Table 4.3, where we plot the convergence rates for the above problem with $\Gamma_{\mathcal{N}} \neq \emptyset$. We chose $\boldsymbol{C}_{12} = (0,0)$ and $C_{11} = 1$ and show the performance for $\mathcal{Q}^3$-elements. The obtained $L^2$-orders are $k + \frac{1}{2}$ and $k$, representing a loss of $\sqrt{h}$. It also worth remarking here that the numerical results in Table 4.3 indicate, in fact, that the rates $k+\frac{1}{2}$ and $k$ proven in [3] for $C_{11} = 1$ and $\boldsymbol{C}_{12}$ arbitrary, but of order one, are sharp.

Thus, the above experiments show that the orders of convergence given by Theorem 2.1 are *sharp* and that the appropriate choice of $\boldsymbol{C}_{12}$ is indeed necessary for this result to hold.

In the following examples we thus always take $\boldsymbol{C}_{12}$ as in (2.11).

**4.2. The effect of the choice of $\boldsymbol{C_{11}}$.** Next, we test the effect of the choice of the coefficients $C_{11}$ on the orders of convergence of the LDG method. We consider the same problem as in the previous experiments, case $\Gamma_{\mathcal{N}} = \emptyset$, and use $\mathcal{Q}^1$- and $\mathcal{Q}^2$-elements. We only show the numerical orders of convergence for the finest grids.

The results are displayed in Tables 4.4 and 4.5. We must compare all these results with those with $C_{11} = 1$ obtained in the first set of experiments. We see that when $C_{11}$ is of order $h^{-1}$, the order of convergence in $u$ remains $k + 1$ but the order of convergence in $\boldsymbol{q}$ degrades from $k + \frac{1}{2}$ to only $k$, as predicted by our analysis; see subsection 3.5.

We also see that taking $C_{11} = h^{-1}$ at the "outflow" boundary and $C_{11}$ of order one elsewhere only results in a slight reduction of the $L^\infty$-orders of convergence.

TABLE 4.6
*Orders of convergence for the LDG method with $C_{11} = 1.0$: $g_{\mathcal{D}} = 0$, $\Gamma_{\mathcal{N}} = \emptyset$.*

| | | $u$ | | $q_1$ and $q_2$ | |
|---|---|---|---|---|---|
| Element | $\ell$ | $L^2$ | $L^\infty$ | $L^2$ | $L^\infty$ |
| $\mathcal{Q}^0$ | 5 | 0.8913 | 0.9278 | 0.9299 | 0.8973 |
| | 6 | 0.9456 | 0.9658 | 0.9662 | 0.9483 |
| $\mathcal{Q}^1$ | 5 | 2.0352 | 1.9750 | 2.0000 | 1.9748 |
| | 6 | 2.0213 | 1.9878 | 2.0003 | 1.9858 |
| $\mathcal{Q}^2$ | 5 | 2.9637 | 3.0266 | 2.9689 | 3.0292 |
| | 6 | 2.9815 | 3.0150 | 2.9855 | 3.0161 |
| $\mathcal{Q}^3$ | 5 | 4.0435 | 3.9806 | 4.0087 | 3.9771 |
| | 6 | 4.0247 | 3.9918 | 4.0041 | 3.9748 |

TABLE 4.7
*Orders of convergence for the LDG method with $C_{11} = 1.0$: $g_{\mathcal{D}}$ quadratic, $\Gamma_{\mathcal{N}} = \emptyset$.*

| | | $u$ | | $q_1$ and $q_2$ | |
|---|---|---|---|---|---|
| Element | $\ell$ | $L^2$ | $L^\infty$ | $L^2$ | $L^\infty$ |
| $\mathcal{Q}^0$ | 5 | 0.9886 | 0.9739 | 0.7359 | 0.0052 |
| | 6 | 0.9935 | 1.0066 | 0.8009 | 0.0142 |
| $\mathcal{Q}^1$ | 5 | 2.0030 | 1.9552 | 1.4906 | 1.0160 |
| | 6 | 2.0015 | 1.9775 | 1.4976 | 1.0091 |
| $\mathcal{Q}^2$ | 5 | 2.9637 | 3.0266 | 2.9689 | 3.0292 |
| | 6 | 2.9815 | 3.0150 | 2.9855 | 3.0162 |
| $\mathcal{Q}^3$ | 5 | 4.0435 | 3.9804 | 4.0087 | 3.9762 |
| | 6 | 4.0245 | 3.9909 | 4.0036 | 3.9717 |

In the remaining cases, we take $C_{11}$ to be of order $h$ in all the domain and then in all but the "outflow" boundary where it is taken to be of order $h^{-1}$. We observe a slight degradation of all the orders of convergence.

These results indicate that the best choice of the stabilization parameter $C_{11}$ for the LDG method on Cartesian grids is to take it of order one, as predicted by our analysis.

**4.3. Piecewise polynomial boundary conditions.** The purpose of these numerical experiments is to show that if the boundary data are piecewise polynomials of degree $k$, the order of convergence of the $L^2$-norm of the error in $\boldsymbol{q}$ is optimal, that is, $k+1$, and not only $k+\frac{1}{2}$ as predicted by Theorem 2.1 and sharp as is shown in subsection 4.1.

We consider two test problems. In the first, we take homogeneous Dirichlet boundary conditions and $f$ such that the exact solution is $u(x_1, x_2) = \cos(\frac{\pi}{2}x_1)\cos(\frac{\pi}{2}x_2)$. In the second, we take piecewise quadratic Dirichlet boundary conditions and $f$ such that the exact solution is $u(x_1, x_2) = x_1^2 + x_2^2 + \cos(\frac{\pi}{2}x_1)\cos(\frac{\pi}{2}x_2)$.

The results of the first problem are reported in Table 4.6 where we can see that the *optimal* order of convergence of $k+1$ for the $L^2$- and $L^\infty$-norms of the errors in *both* $u$ and $\boldsymbol{q}$ are obtained; the results for $k = 0, 1, 2, 3$ are displayed.

The results of the second problem are reported in Table 4.7, where we see that the *optimal* order of convergence of $k+1$ for the $L^2$- and $L^\infty$-norms of the errors in *both* $u$ and $\boldsymbol{q}$ are obtained for $k \geq 2$, as claimed. For $k < 2$, the order of convergence in the

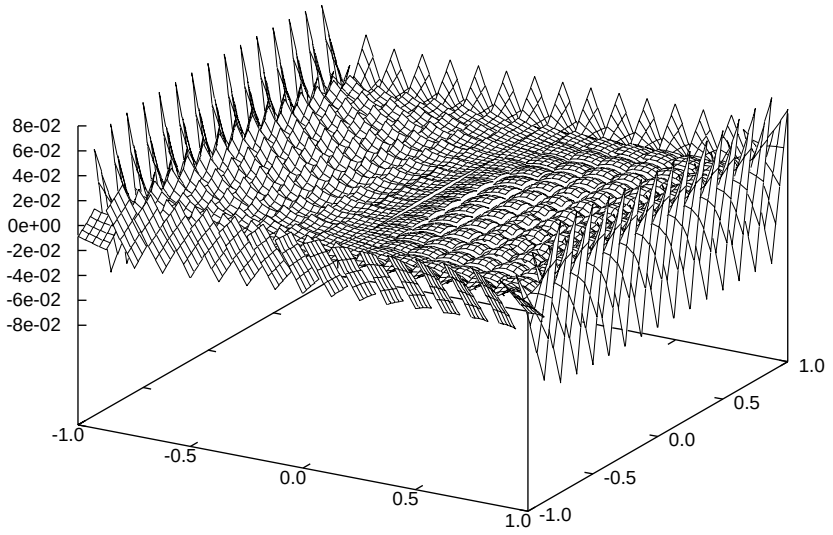


FIG. 4.1. *The error in the first component of the gradient for* $\mathcal{Q}^1$*:* $g_{\mathcal{D}}$ *quadratic,* $\Gamma_{\mathcal{N}} = \emptyset$.

$\mathrm{L}^2$-norm of the error in $\boldsymbol{q}$ is $k + \frac{1}{2}$ only, which is nothing but the order of convergence predicted by Theorem 2.1.

To better understand this phenomenon, we plot the errors in $q_1$ for $\mathcal{Q}^1$- and $\mathcal{Q}^2$-elements in Figures 4.1 and 4.2, respectively; the triangulation has $16 \times 16$ elements and corresponds to the index $\ell = 4$. We immediately see the oscillatory behavior of the error typical of finite element methods. In Figure 4.1, we see that the error obtained with $\mathcal{Q}^1$-elements is bigger at the boundary than at the interior. This, together with the fact that the order of convergence in $\mathrm{L}^2$ is $\frac{3}{2}$ whereas the order of convergence in $\mathrm{L}^\infty$ is only 1, suggests that the error at the boundary is a factor of order $h^{-\frac{1}{2}}$ bigger than the error at the interior of the domain. On the other hand, the behavior of the error with $\mathcal{Q}^2$-elements is rather different, as can be seen in Figure 4.2. Indeed, the error behaves in the same way at the boundary and at the interior; this is further confirmed by the fact that both the order of convergence in $\mathrm{L}^2$ and the one in $\mathrm{L}^\infty$ are equal to $k + 1$.

These experiments justify our contention that the optimal order of convergence in $\boldsymbol{q}$ can be reached if the boundary conditions are piecewise polynomials of degree $k$. Our theoretical analysis does not explain this phenomenon.

**4.4. A three-dimensional example.** In this experiment, we consider the elliptic model problem (1.1) on the three-dimensional domain $\Omega = (-1, 1)^3$. We take Dirichlet boundary conditions and $f$ such that the exact solution is

$$u(x_1, x_2, x_3) = x_1^2 + x_2^2 + x_3^2 + \cos\left(\frac{\pi}{2}x_1\right)\cos\left(\frac{\pi}{2}x_2\right)\cos\left(\frac{\pi}{2}x_3\right).$$

The results are displayed in Table 4.8; the computation on level 5 with $\mathcal{Q}^2$-elements did not fit into the computers available to us. We can see that the orders of convergence

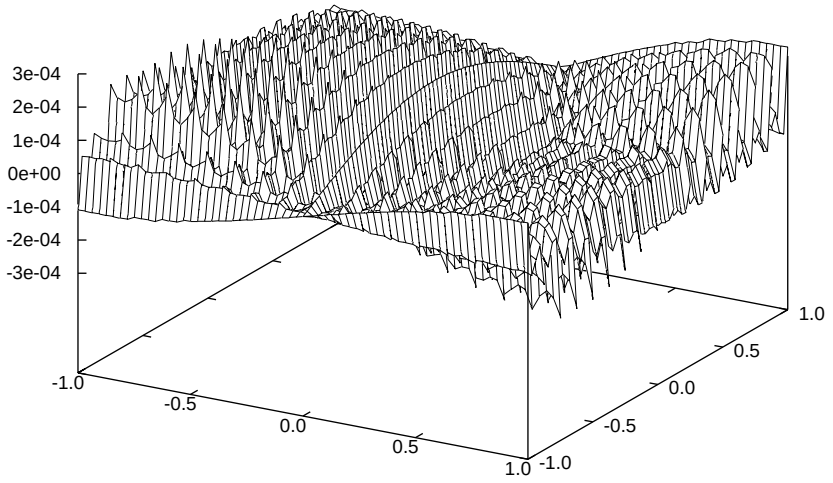


FIG. 4.2. *The error in the first component of the gradient for* $\mathcal{Q}^2$*:* $g_{\mathcal{D}}$ *quadratic,* $\Gamma_{\mathcal{N}} = \emptyset$.

TABLE 4.8
*Orders of convergence for the LDG method with* $C_{11} = 1.0$ *in 3D:* $g_{\mathcal{D}}$ *quadratic,* $\Gamma_{\mathcal{N}} = \emptyset$.

| | | $u$ | $q_1$ and $q_2$ |
|---|---|---|---|
| Element | $\ell$ | $L^2$ | $L^2$ |
| $\mathcal{Q}^0$ | 3 | 0.9389 | 0.5118 |
| | 4 | 0.9367 | 0.6177 |
| | 5 | 0.9452 | 0.7203 |
| $\mathcal{Q}^1$ | 3 | 1.8573 | 1.3374 |
| | 4 | 1.9278 | 1.4345 |
| | 5 | 1.9636 | 1.4723 |
| $\mathcal{Q}^2$ | 3 | 2.9204 | 2.8642 |
| | 4 | 2.9326 | 2.9338 |
| | 5 | n/a | n/a |

are similar to those obtained in the corresponding two-dimensional test problem in the previous subsection; cf. Table 4.7. This gives an indication that the orders of convergence of the LDG method in three space dimensions behave in the same way they do in the two-dimensional case.

**5. Concluding remarks.** In this paper we have shown that the LDG method on Cartesian grids and with a special numerical flux superconverges; the proof of this result is based on suitable defined projections $\mathbf{\Pi}$ and $\Pi$ exhibiting a tensor product structure. This work extends the corresponding result by LeSaint and Raviart [8] for the DG method for linear hyperbolic problems and that by Castillo [2] and Castillo, Cockburn, Schötzau, and Schwab [4] for the LDG method applied to the

one-dimensional transient convection-diffusion. Extensions of this work to more general elliptic and both steady and transient convection-diffusion problems can easily be made.

**Acknowledgment.** We would like to thank the reviewers for their valuable comments and suggestions.

## REFERENCES

[1] W. Bangerth and G. Kanschat, *Concepts for Object-Oriented Finite Element Software—The* `deal.II` *Library*, Report 99-43, Sonderforschungbereich 3-59, IWR, Universität Heidelberg, Heidelberg, Germany, 1999.

[2] P. Castillo, *An optimal error estimate for the local discontinuous Galerkin method*, in Discontinuous Galerkin Methods: Theory, Computation and Applications, B. Cockburn, G.E. Karniadakis, and C.-W. Shu, eds., Lect. Notes Comput. Sci. Eng. 11, Springer-Verlag, Heidelberg, 2000, pp. 285–290.

[3] P. Castillo, B. Cockburn, I. Perugia, and D. Schötzau, *An a priori error analysis of the local discontinuous Galerkin method for elliptic problems*, SIAM J. Numer. Anal., 38 (2000), pp. 1676–1706.

[4] P. Castillo, B. Cockburn, D. Schötzau, and C. Schwab, *An optimal a priori error estimate for the hp-version of the local discontinuous Galerkin method for convection-diffusion problems*, Math. Comp., to appear.

[5] P. Ciarlet, *The Finite Element Method for Elliptic Problems*, North-Holland, Amsterdam, 1978.

[6] P.G. Ciarlet and P.A. Raviart, *General Lagrange and Hermite interpolation in $R^n$ with applications to finite element methods*, Arch. Ration. Mech. Anal., 46 (1972), pp. 177–199.

[7] B. Cockburn and C.-W. Shu, *The local discontinuous Galerkin method for time-dependent convection-diffusion systems*, SIAM J. Numer. Anal., 35 (1998), pp. 2440–2463.

[8] P. LeSaint and P.A. Raviart, *On a finite element method for solving the neutron transport equation*, in Mathematical Aspects of Finite Elements in Partial Differential Equations, C. de Boor, ed., Academic Press, New York, 1974, pp. 89–145.

[9] D. Schötzau and C. Schwab, *Time discretization of parabolic problems by the hp-version of the discontinuous Galerkin finite element method*, SIAM J. Numer. Anal., 38 (2000), pp. 837–875.